Interface strength in glass fibre-polypropylene measured using the fibre pull-out and microbond methods

L. Yang & J. L. Thomason

University of Strathclyde, Department of Mechanical Engineering, 75 Montrose Street, Glasgow G1 1XJ, United Kingdom.

Abstract

Interface strength in glass fibre-polypropylene was measured using both fibre pull-out and microbond methods. Excellent correlation between two methods was obtained. Data from microbond test could be divided into two groups according to whether or not there was constant interfacial friction after debonding. Microscopy observation on tested microbond samples which had exhibited decreasing interfacial friction after debonding revealed considerable residual resin around the debonded area of samples. Further investigation indicated that this unexpected difference was caused by the variation in mechanical properties of the matrix due to thermal degradation during sample fabrication.

Keywords: A Glass fibre, A Thermoplastic resin, B Adhesion, D Mechanical testing

Introduction

Use of glass fibre-reinforced thermoplastic polymer composites has been rapidly increasing in a great many applications due to their high performance, mass processability and recyclability [1]. It is well known that the mechanical properties of fibre-reinforced thermoplastic composites are strongly affected by factors such as fibre length, fibre concentration [2,3], and state of the interface [4,5] between the fibre and the matrix. In particular, optimisation of the fibre-matrix interface is important to achieve the desired performance in composite materials because it is responsible for transferring the applied load onto the load bearing fibres. Ample literature on interface phenomena and related aspects intimate the fact that the interfacial region is very complex as well as significantly important. It is particularly true when the early concept of the interface from a two-dimensional plane is extended into a three-dimensional interphase between bulk fibre and bulk matrix [6]. This complex region has also been established between the silane-sized glass fibre and the maleic anhydride modified PP [4,7]. Over the years there have been tremendous efforts to, develop adequate techniques which could characterise fibre-matrix adhesion levels in composites, identity appropriate interfacial parameters which could represent actual mechanisms of interface failure, and provide applicable theoretical models which could explain the experiment results. These aspects have been thoroughly reviewed [8,9]. One of the generally accepted manifestations of adhesion is the mechanically measured value of interfacial shear strength (IFSS or τ). A number of direct micromechanical methods (i.e. testing samples involving a single fibre) have been developed to determine the IFSS. These include the single fibre pull-out test [10], the microbond test [11], the push-out test [12] and the single fibre fragmentation test [13]. The microbond technique has been extensively employed to characterise the adhesion levels of thermosetting composites

due to its capability of working with the relatively small embedded length necessary to deal with strong adhesion between fibre and matrix [14]. To a lesser extent, this method has also been applied to thermoplastic systems [15-17]. It is often seen that the fitting line based on linear least square method to the data in load-embedded area plots obtained using the microbond test does not actually pass through the origin [18]. This means that the average interfacial shear strength could be highly affected by the range of embedded length of experimental specimens. The embedded length, thus, is desired in a range as broad as possible in this circumstance. The single fibre pull-out test has been used widely to evaluate the IFSS for thermoplastic composites such as glass fibre-reinforced polypropylene (GF-PP) [4,5,7,19], where a relative low value of adhesion is expected. The embedded length L_e in this method can extend into a much broader range compared with the microbond test and is limited by the fibre strength σ_f, the fibre diameter D, and the interfacial shear strength τ via the Eq. 1

$$L_e < \frac{\sigma_f D}{4\tau} \qquad (1)$$

For bare glass fibres (i.e. no any coating or sizing on the fibre) with a gauge length of 8 mm and diameters in the range of 15-21 μm, the average fibre tensile strength could be ~ 1.5 GPa. Given that the bare glass fibre IFSS is ~3-6 MPa for neat isotactic PP (i.e. polypropylene homopolymer without any additional modification other than the routine additives such as stabilisers) this means that a maximum embedded length of approximately 2.5 mm can be successfully tested without fibre failure. Such a limit may also be applicable to sized GF since the use of sized glass fibre usually involves modified PP in order to improve the adhesion of GF-PP and the increase of fibre strength brought about by the sizing could be cancelled out by the similar order of increase in the adhesion. It is also well known that there is a considerable distribution in the fibre diameter for commercial GF. For the diameters range given above, the average fibre diameter could be around 17.5μm. This means that anyone who intends to employ

the single fibre pull-out test to efficiently generate data related to interfacial failure should keep the average embedded length less than 2.2 mm. In addition, a free fibre length longer than 8mm and extra handling during sample preparation and testing could further lower the limit to the testable fibre embedded length.

Consequently the combination of these two methods, therefore, could be chosen as an effective approach to evaluate IFSS of GF-PP. Currently there seems to be no overall consensus among these techniques and large scatter in the experimental results seems to be a common issue, which has been inhibiting the development of effective data reduction [20]. In addition, it appears that although some of these micromechanical techniques have been extensively compared in thermosetting composites this is not the case for thermoplastic systems. Sample preparation for these techniques is not optimised for use with thermoplastic matrices [21], nevertheless comparing results obtained by different measurement methods should provide a better understanding of interfacial behaviour in thermoplastic composites. The present work focuses on this interest and tries to gain an improved understanding of correlation between the interfacial properties of GF-PP, the experimental procedures, and data variation in the experimental results. The microbond and fibre pull-out methods have been employed to measure the interface strength of GF-PP over a wide range of embedded length from 130μm up to 1500μm.

Experimental

In this work, we have limited ourselves to the system consisting of boron free bare E-glass fibre from Owens Corning with the average fibre diameter of 17.4μm and isotactic homopolymer polypropylene [SABIC®PP 579S] with the melt flow index value equal to 47 determined at 230ºC and 21.6N (PP47). The fibre strength was determined by using

the single fibre tensile test based on ASTM D3379-75. Individual fibres were glued onto card tabs with a central cutout that matched the gauge length chosen for the test. Then the tab ends were gripped by the universal testing machine (Instron® Model 3342).

After the specimen had been mounted in the test machine, a section of the tab was carefully cut away, leaving the specimen free to be loaded during the test. The gauge length of 10mm close to the free fibre length of 7mm in both microbond and single fibre pull-out tests was chosen and approximate a hundred of specimens were tested.

There seems to be no standard way of using thermoplastic polymers to make samples for either the single fibre pull-out or the microbond test. Every laboratory, thus, has developed their own methods with essentially the same idea and different procedures. The method developed in this work is presented as follows. The same card frames used in the single fibre tensile test were employed as the sample holders for the microbond and single fibre pull-out test as shown in Fig. 1. A slightly different method from the one that has been adopted in other works to form droplets on a single fibre [8] is illustrated in Fig. 2. A single fibre first was glued at the contact points between the fibres and the window cut. Then a small piece of PP47 fibre was transferred on the surface of the suspended glass fibre. The PP47 fibre loosely hung on the fibre and could shake off easily. Thus a soldering iron was used to slightly heat the PP47 fibre so that it could firmly coil itself around the glass fibre. Finally a number of samples as the entire assembly displayed in Figure 1 were transferred together into an oven at a temperature of 220ºC well above the melting temperature of PP47 to ensure complete melting and to remove any thermal history. The time for specimens being retained in the oven was set to 4 min because 2 and 3 min proved too short to form enough testable droplets and thermal degradation during the droplet formation at elevated temperature could complicate the measurement if it is too long. The samples eventually cooled down to

ambient temperature and were then screened under Nikon Epiphot Inverted optical microscope before each microbond test. Only well-shaped, symmetrical droplets were selected for the experiments. The droplet size including droplet length (i.e. embedded length L_e) and droplet diameter and fibre diameter were measured to determine the embedded area of the fibre as shown in Fig. 3.

To perform the microbond test, a device was manufactured [22], with two movable knife edges controlled by a pair of micrometer heads with resolution to 1μm (see Fig. 4). The microbond tests were conducted with a free distance between fibre and knife edge of 20μm. A stereo-microscope was utilised to aid the positioning of knife edges and monitor the testing process. The same testing machine used in the single fibre tensile test with 10N load cell was employed to carry out the test with the rate of fibre end displacement set to 0.1mm/min. The fibre with bonded resin droplets was mounted in the machine. Some card frame was left taped to the bottom of the fibre to keep it under tension (~0.5mN). The fibre was pulled out of the droplet while the droplet was constrained by the knife edges as shown in Fig. 4. The load-displacement for each test was recorded to obtain the peak load, F_{max}, which, along with the corresponding fibre diameter and embedded length was used to calculate the IFSS according to Eq. 2. The tested samples were examined under the microscope again to see if pure debonding process had occurred. Approximate 30 single tests were conducted to obtain the average IFSS.

$$\tau = \frac{F_{\max}}{\pi D L_e} \qquad (2)$$

For single fibre pull-out test, PP47 films were sliced into strips with different widths, which would roughly determine the embedded length. A glass fibre was quickly

embedded in the matrix on a hot plate and at last the resin block with embedded fibre was transferred on the card as shown in Fig. 1. When the PP47 was melted under the same thermal conditions as in droplet formation for microbond tests, it could penetrate into the card and formed a strong bond with it. Each card provided two samples for its own test respectively. Single fibre pull-out tests were conducted with the same testing rate as in microbond tests (see Fig. 5). The card with two samples on it was cut through the middle into two halves. The bottom margin of either half was gripped by a clamp. The fibre was then pulled out of the matrix. The load-displacement curve for each sample was recorded for each test. The pulled out fibres were also examined under the same microscope to see if there is any residual resin left behind on the fibre. From each force-displacement curve the peak force $F_{\max}$ and the embedded length, L_e, were obtained and the IFSS is calculated using the same the Eq. (2). Over 20 tests were conducted to obtain the average IFSS.

Results and discussion

Over the course of the investigation, approximately 1000-bare glass fibres were measured using the optical microscope to establish a profile for the fibre diameter and its distribution. An average fibre diameter of 17.4μm was obtained. Fig. 6 shows that the presence frequency of this mean value is actually only 21% within a fairly broad distribution. 60% of fibres have a diameter less than or equal to17.4μm. This indicates that it is very likely to encounter fibre breakage rather than fibre pull-out in the single fibre pull-out test when the embedded length above 2.2 mm as discussed above. In addition, the average fibre tensile strength of 1.5±0.3GPa at 10 mm gauge length was obtained by the single fibre tensile test. Fig. 7 shows fibre strength distribution approximated by the two-parameter Weibull distribution. It can be seen that there is a reasonably good agreement between experimental data and Weibull distribution. The

Weibull modulus equal to 5 is obtained from the slope of the fitting line in the Weibull plot.

A plot of peak force vs. interfacial area is shown in Fig. 8 for the data set obtained with bare GF in neat PP47 by the single fibre pull-out method. A straight line was fitted to the data and forced to go through the origin according to Eq. (2), resulting in a value of the IFSS 3.3 MPa from the slope of this line. This agrees well with the IFSS-range (3-6 MPa) published in the literature for GF-iPP by using the single fibre pull-out technique [4,5,7,19]. It is seen that the data points fall on the straight line with relatively little scatter. Post microscopy inspection shows that there is no residual resin left behind around the debonded area of fibres indicative of likely clean interfacial failure. Although the value of R^2=0.82 for the dotted line in Fig. 8 indicates a good correlation between experimental data and Eq. 2, it can be seen that a higher value of R^2=0.85 is obtained when not forcing a fitting line (i.e. solid line) to pass through the origin.

A plot of peak force vs. embedded area is obtained by the microbond method is shown in Fig. 9 for the data set with bare GF in PP47. The data can apparently be divided into two groups according to whether there is constant or decreasing dynamic friction after debonding. This division seems to be related to the droplet size. Relatively small resin droplets are more likely to give decreasing dynamic friction whereas larger droplets exhibit constant friction after debonding. Interestingly these two groups also appear to fall on similar trend lines as shown by the solid fitting lines, which certainly do not go through the origin. Further microscopy observation of tested specimens from microbond tests has divided these two distinctive situations into two categories (A and B) as shown in Figs. 10 and 11. About 2-7 micrometres thickness of residual resin was observed around the debonded area of the fibres in group B, which corresponds to decreasing

friction after the peak load as seen in Fig. 11. Very occasionally tested samples exhibiting category A behaviour were also observed with residual resin but at a much lower level. Most samples in the category A exhibited a clean debonded fibre surface after the test. According to further observation on matrix indentations caused by knife edges (see Fig. 12), such a difference did not arise from the knife edges, which were spaced 20μm away from each side of the fibre throughout all tests. In addition, the fracture surfaces exposed via the indentation are different between two categories and samples in category A undertaking a higher peak load exhibited a less severe indentation compared to those in category B with the similar embedded area. These observations may imply that this difference between these two groups is due to variation in mechanical properties of the matrix. The failure mode in B is usually referred to as cohesive matrix failure while in A is termed that as adhesive interfacial failure. The former is generally considered to be clearly indicative of good adhesion relative to the latter due to some interfacial modification made in the same work [5,17]. However, in this case there had been no modification of the interface in any case, implying all samples should exhibit a similar level of adhesion. Cohesive matrix failure may also be caused by deterioration of mechanical properties of the matrix, from which good adhesion with fibres could hardly be expected. Thus we must seek an explanation for these different behaviours of the test parameter.

Consequently another set of microbond tests was conducted with variation of the thermal history in matrix by changing its duration of stay in the oven from 4 min to 6 min at the same temperature (i.e. 220°C). The results are shown in Fig. 13. It can be seen that the extra 2 min heating has made a significant impact on the IFSS value obtained for bare GF and neat PP47 studied in the present work. The 6 min set has an overall lower peak load than the 4 min in the same range of droplet size. Few tested

samples in category B could be found in the 4 min data set, while about half of tested samples appears as category B in the 6 min group. In both data sets the tested samples in the category B tend to emerge from relatively small droplets. As droplet size increases it becomes more likely to have tested samples in category A. In comparison with two data sets, such a tendency has also been modified by different thermal loads. It should be noticed that there seems to be a non-linear increase in the 6 min group, of which the largest droplets tend to return to the 4 min data set trend. It can be seen that the additional thermal load has not only changed adhesive interfacial failure into cohesive matrix failure but also considerably reduced the value of IFSS. The average values of sum of individual IFSS for different categories of microbond specimens in both 4 and 6 min sets are shown in Fig. 14. It can be seen that the additional 2 min heating has lowered the average value in the 4 min-category A set from 2.3 MPa down to 1.6 MPa in the 6 min-category A and the value in the 4 min-category B from 1.2 MPa to 0.7 MPa in the 6 min-category B. Statistic analysis of the data in Fig. 14 using the Two Sample *t*-test indicated that the reduction in average IFSS by both increased treatment time (4 min vs 6 min with fixed category) or a change of category (A vs B at fixed treatment time) was statistically significant at the 95% confidence level. Tested samples in category B of both sets generate the values in Fig. 14 around the shear yielding strength (~1 MPa) for atactic polypropylene [17], exhibit residual resin on the tested fibres, and apparently possesses a weaker region in the matrix with respect to the interface.

The results of the IFSS and microscopy observation indicate that the variation in thermal conditions has strongly influenced the properties of the matrix. To examine this possibility, the embedded length normalised maximum slopes of load-extension curves recorded in microbond tests were estimated. Individual IFSS values vs. maximum slopes of corresponding load-displacement curves are plotted in Fig. 15. The free fibre length was kept approximately the same throughout all tests as shown in Fig. 1. Thus

the variation in slope of the load-extension curve of the experiments should reflect changes in matrix stiffness, assuming the compliance of all other parts in the testing fixture remain the same. It can be seen in Fig. 15 that the measured IFSS tends to rise as the slopes of load-extension curves increase in both groups and overall, samples in category A of two groups with higher IFSS values also have higher slopes than those in category B. It is noticed that the situation in Fig. 15 is analogous to that in Fig. 13. Indeed, the fact that the data in Fig. 13 clearly deviate from the origin and tend to intersect the axis of embedded area means that apparent IFSS increases as the increase in embedded area, or droplet size neglecting the variation in fibre diameter. Thus the combination of these two observations implies that the slope of load-extension curve increases as the droplet becomes bigger as shown in Fig. 16. Consequently it appears that there may be a correlation between the IFSS and the PP stiffness.

One possible explanation for these observation can be found in terms of a variation in matrix mechanical properties due to thermal oxidation and degradation. Small polypropylene droplets are naturally more vulnerable to thermal degradation and more sensitive to oxidative attack at elevated temperature due to their relative high surface to volume ratio. Thus when the droplets with various sizes undergo the same thermal loads, the small ones may suffer from more severe thermal oxidation and even thermal degradation. As the tacticity along the polymer chain is reduced by either the addition of oxygen atoms on polymer chains or chain breakage, the degree of crystallinity can be expected to decrease. As a result, in both the 4 min and the 6 min sets the decrease in crystallinity caused by thermal degradation during sample fabrication could lead to the degradation of PP47 mechanical properties. For relatively small droplets, this deterioration of mechanical properties was so severe that PP47 shear strength could be less than its interface strength with glass fibre, and cohesive matrix failure would then

occur. As the droplets become bigger, it would be more possible for them to maintain sufficient crystallinity and in turn mechanical properties, which would provide a matrix shear strength higher than its interface strength with fibre. Interfacial failure would then have a higher probability to occur. When the thermal process was relatively mild (e.g. 4 min at 220°C), those droplets that would have failed in the matrix under a severe condition (e.g. 6 min at 220°C) were able to maintain sufficient mechanical properties and prevent the matrix failure during the test. Unlike most glass fibre-thermosetting systems, there may be little or no chemical reaction across the interface between the bare GF and neat PP [5]. The compressive radial stress built around the interface during fabrication of thermoplastic composites is regarded as the major contribution to the stress transfer capability at the interface [23,24]. The level of this radial stress at the interface depends on processing conditions and physical properties of the fibre and the matrix such as their stiffness and thermal expansion coefficients. Although it is known that for most crystalline polymers, thermal expansion is depressed by crystal lattice constraints, in a thermoplastic polymer thermal expansion is strongly influenced by the strength of the secondary bonds between molecules [25]. For instance, thermoplastic polymer molecules held together by strong hydrogen bonds generally expand less than those held by dispersion bonds [25]. Therefore if more severe thermal degradation had happened to samples in the 6 min group, there would be much more amount of oxygen atoms in polymer molecules held together by strong hydrogen bonds between those polar atoms. This could lead to relative small radial compressive stress at the interface of samples in the 6 min group and in turn lower IFSS values than those in the 4 min group. In addition, less crystallinity in the 6 min group may imply potential radial stress relaxation of the matrix, which does not favour high IFSS.

Finally the results of measurements of the IFSS of bare GF and neat PP47 obtained

using the single fibre pull-out and microbond methods are presented together in Fig. 17. Excellent agreement on the conventional data-reduction technique (e.g. the averaged IFSS) between two methods was obtained. Here the fitting lines were not forced through the origin because it is supposed that they would tend to do so if there was no reduction in IFSS caused by the thermal oxidation and/or degradation as explained above. In fact the deviation of the peak load vs. embedded length line to intersect the embedded length axis at a non-zero value is exactly what would be expected from the previous discussion if reducing the embedded length (i.e. the size of the PP droplet) leads to an increase in the thermal degradation of the PP and a consequent lowering of the apparent IFSS (either by a lowering of the actual interfacial strength or a transition to a matrix dominated failure). In this case, the good correlation between the two methods may imply that samples in the single fibre pull-out test were also affected by thermal degradation, although to a lesser degree than those in the micrbond test. Consequently, apparent IFSS seems to be an adequate quantitative parameter which can characterise the mechanism of interfacial failure in the bare GF- neat PP47 system studied in the present work.

Conclusions

Interface strength in bare GF-PP47 has been measured using both fibre pull-out and microbond methods. Excellent correlation between two methods was obtained. This implies that apparent IFSS is an adequate quantitative parameter which can characterise the mechanism of interfacial failure in glass fibre-thermoplastic composites. In addition, IFSS values of 3-4 MPa for bare GF and PP47 were obtained, which lie in the range of 3-6 MPa in the literature for bare GF-neat PP. It was found that the data from the microbond test could be divided into two groups according to whether or not there was constant interfacial friction after debonding. Further investigation revealed that such a

division could be interpreted by the difference in physical properties of the matrix due to the effect of thermal oxidation and degradation on the polymer matrix. It is concluded that this effect can interfere with the IFSS measurement of GF-PP and complicate the data reduction. Thermal deterioration was also found to reduce not only the mechanical properties of the matrix as expected, but also the IFSS between the fibre and the matrix. This conclusion is indirectly supported by the correlation between the IFSS and the compliance of fibre-polymer , which is assumed to vary in accord with the variation of the matrix compliance. Thus it is highly recommended to take into account the effect of thermal deterioration on the IFSS measurement of GF-PP, especially for the microbond method. Further work will focus on providing direct evidence for this hypothesis.

Acknowledgements

The authors would like to thank Chris Cameron for manufacturing the microvise and James Kelly and Peter Chung for the assistant with microscopy measurements.

List of Figures

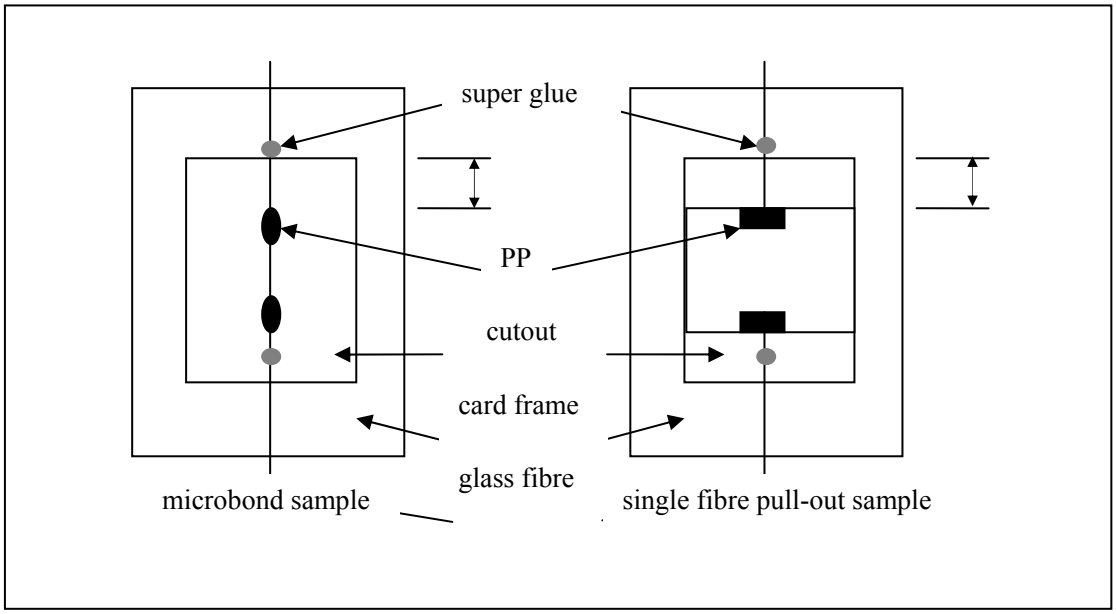

Fig. 1 Schematic representation for single fibre specimen

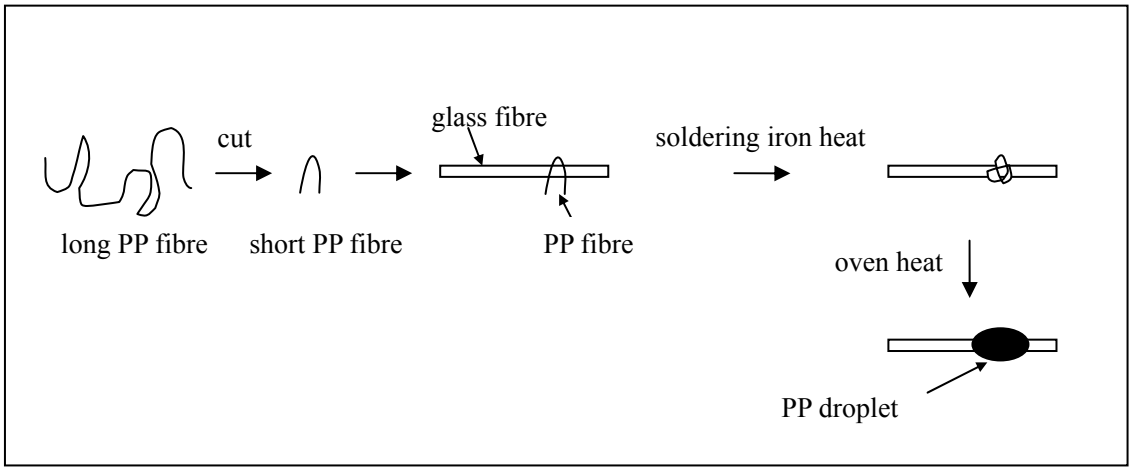

Fig. 2 Procedure to form PP droplet on the glass fibre

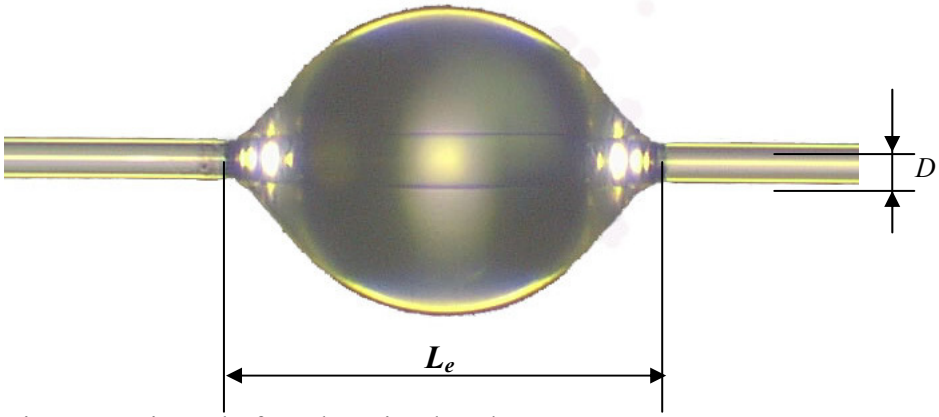

Fig. 3 Specimen before the microbond test

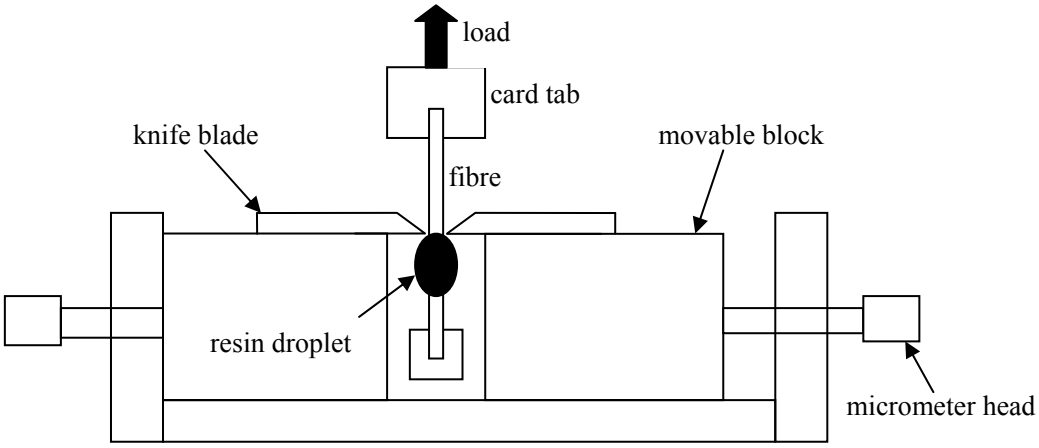

Fig. 4 Schematic illustration of microvise: not to scale

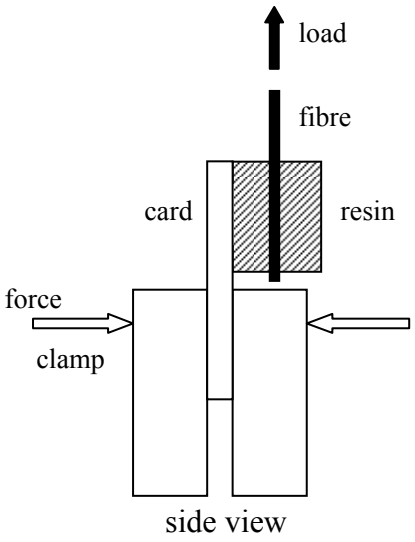

Fig. 5 Schematic representation of fibre pull-out test: not to scale

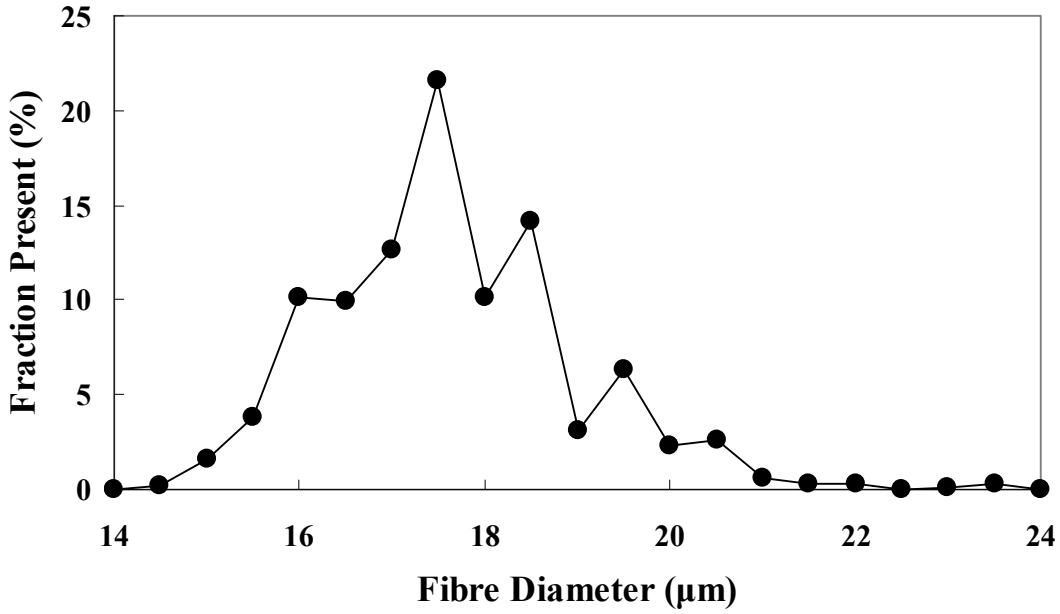

Fig. 6 Diameter distribution of bare glass fibre

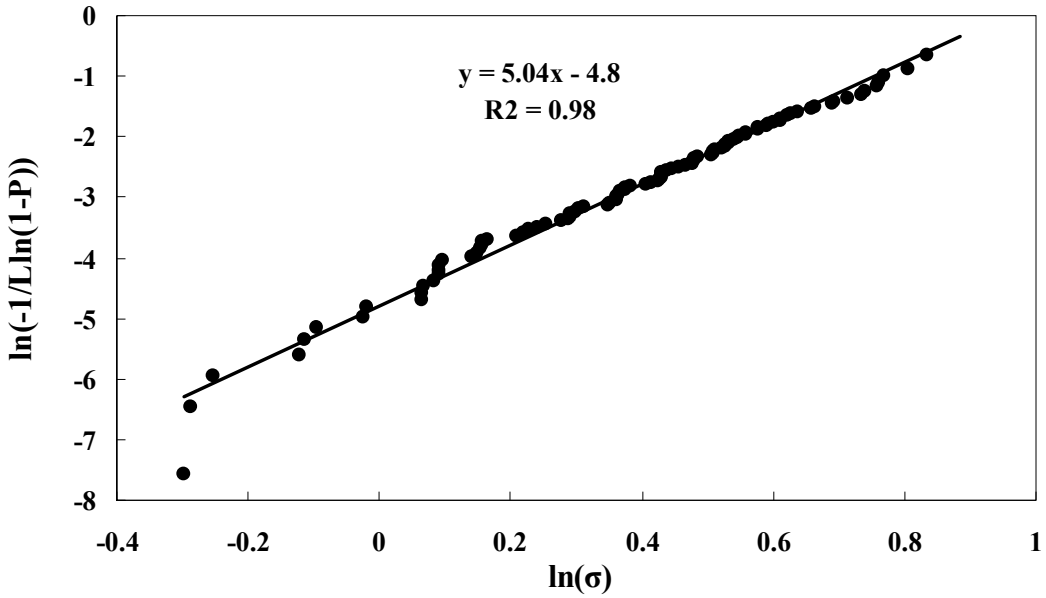

Fig. 7 Single fibre tensile test results in Weibull coordinates for 10 mm gauge length; solid line corresponds to Weibull strength distribution

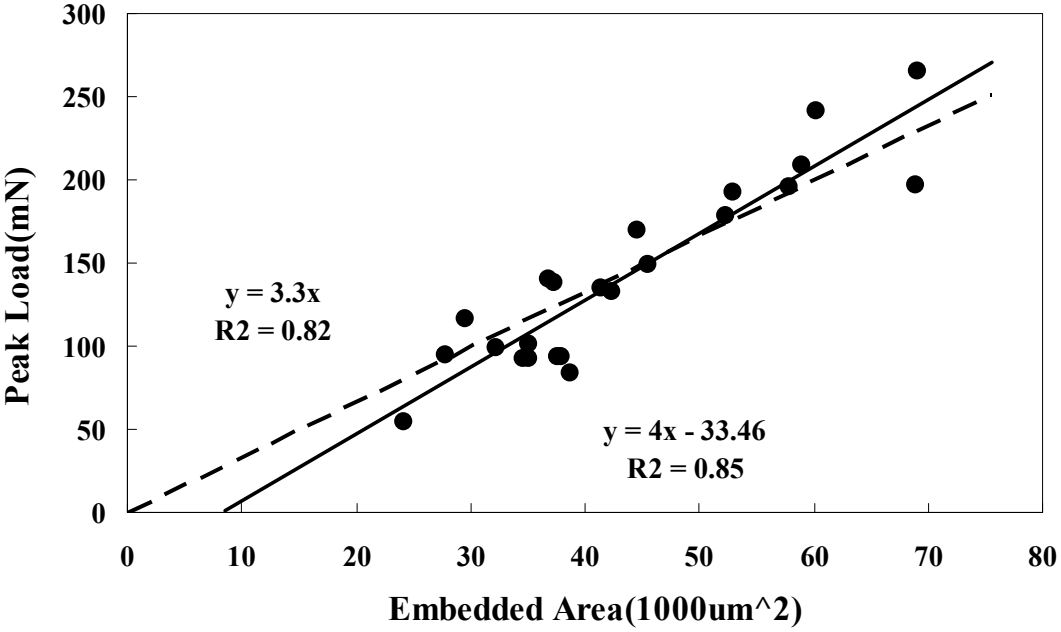

Fig. 8 Plot of peak force vs. embedded area measured for bare GF in PP47 using single fibre pull-out test

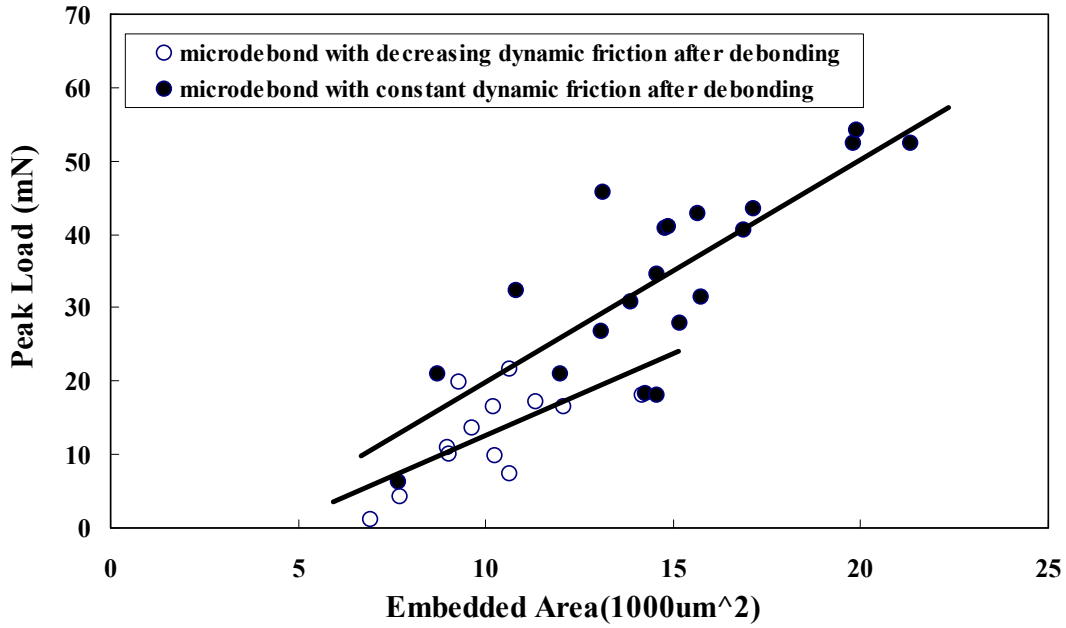

Fig. 9 Plot of peak force vs. embedded area measured for bare GF in PP47 using microbond test

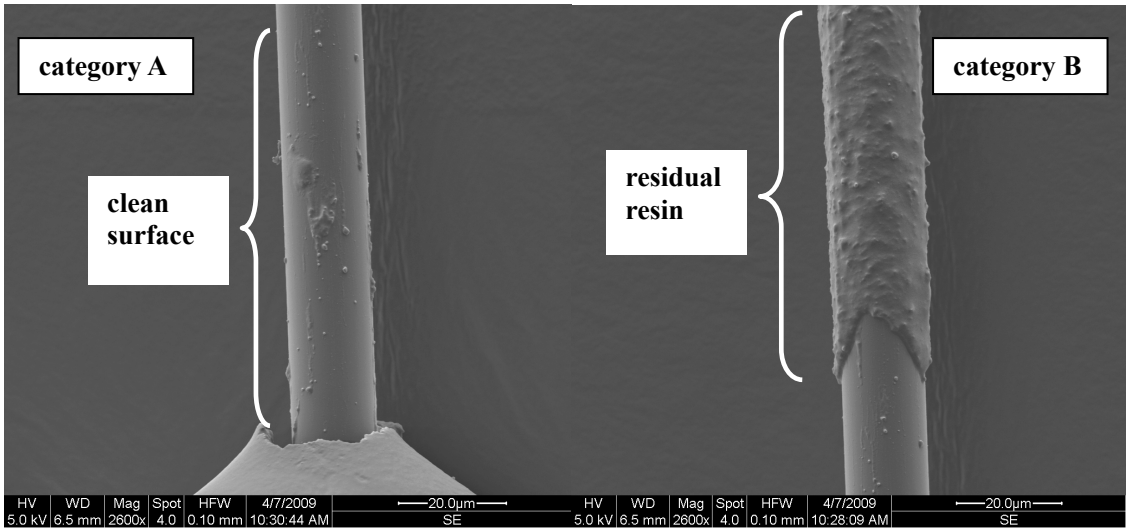

Fig. 10 SEM photograph of different debonded fibre surfaces

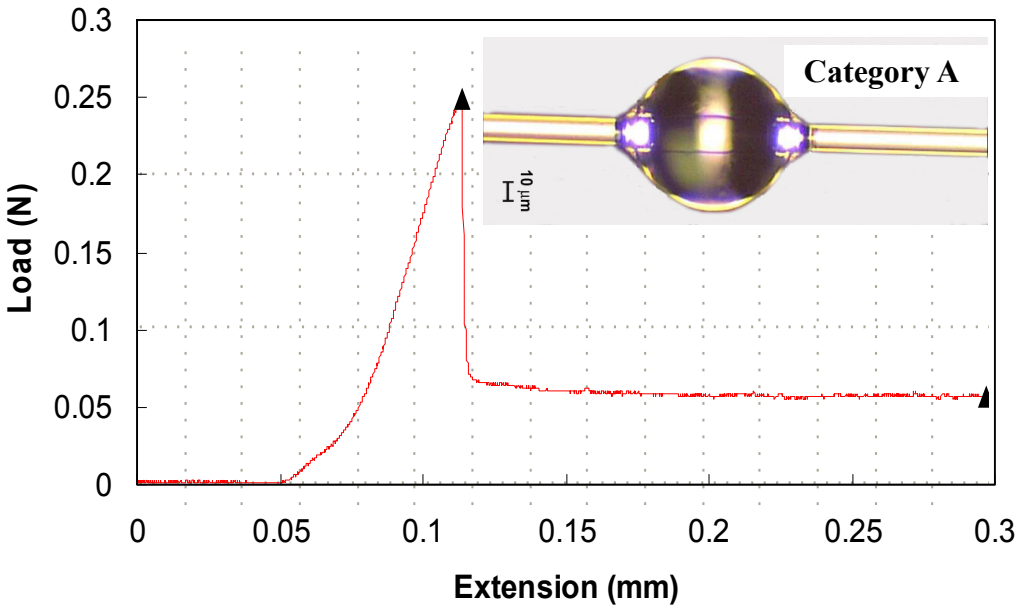

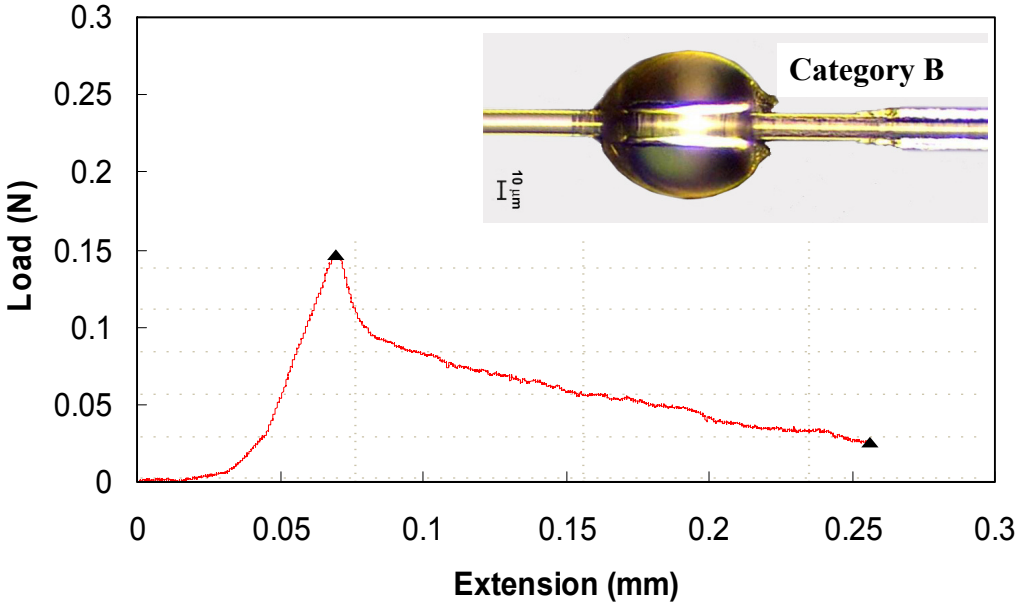

Fig. 11 Typical load vs. extension plots of tested samples of category A and category B recorded in the microbond test

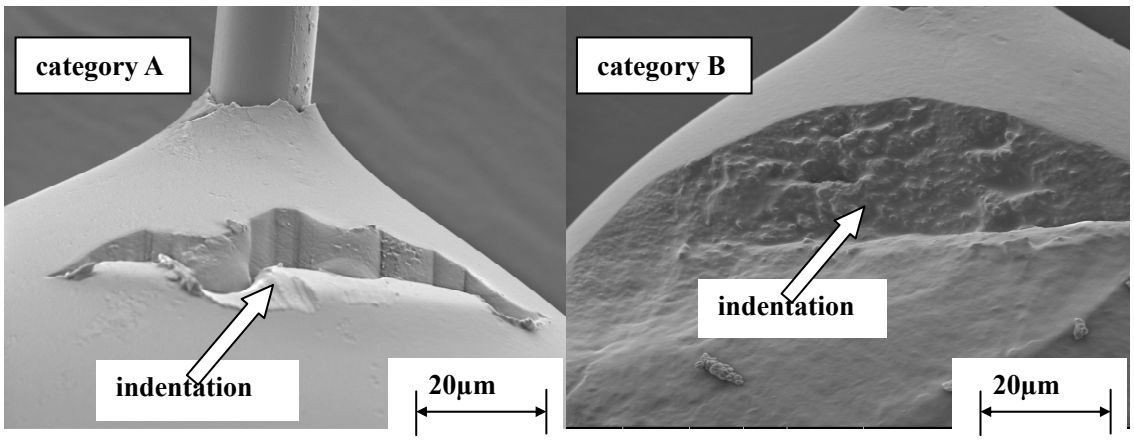

Fig. 12 SEM photograph of different indentations caused by knife edges

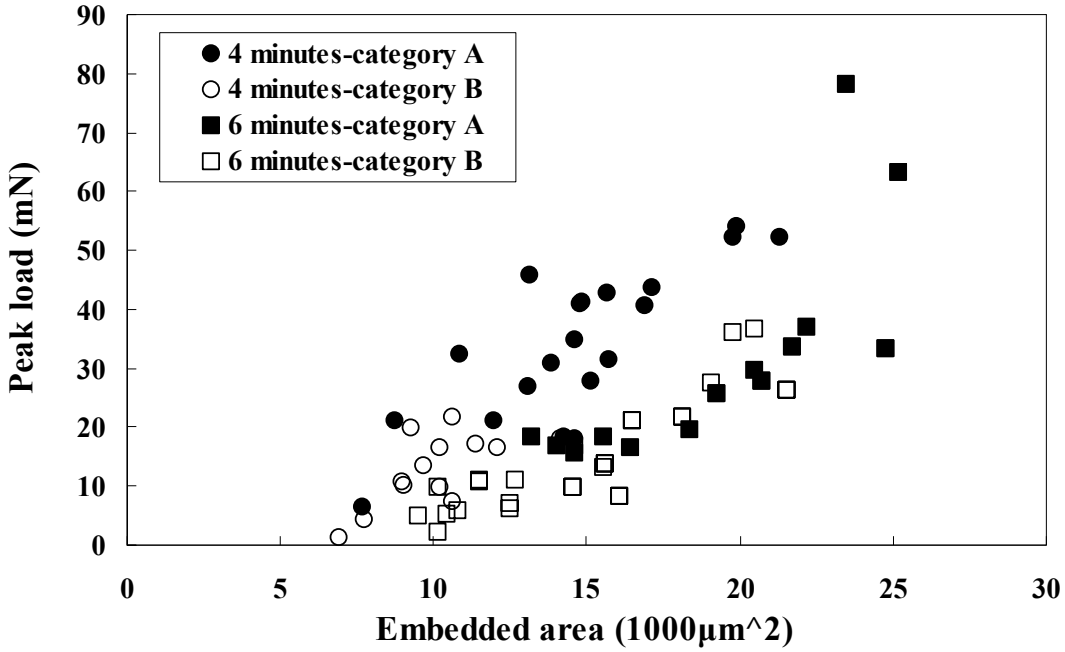

Fig. 13 Comparison of effect of different thermal loads on the IFSS of bare GF-PP47 measured using microbond method

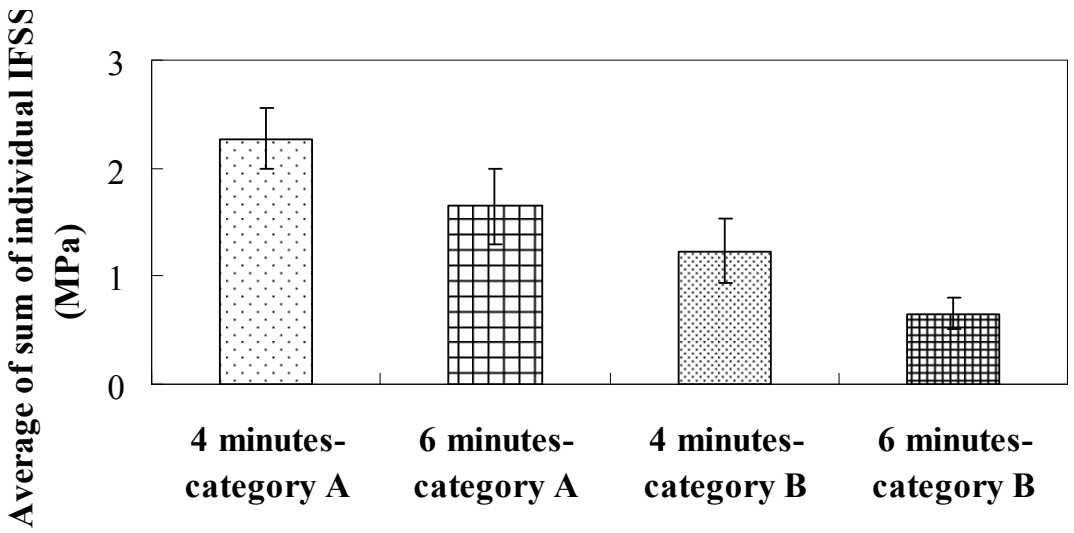

Fig. 14 Comparison of average values of sum of individual IFSS between different categories of microbond samples in 4 and 6 min groups

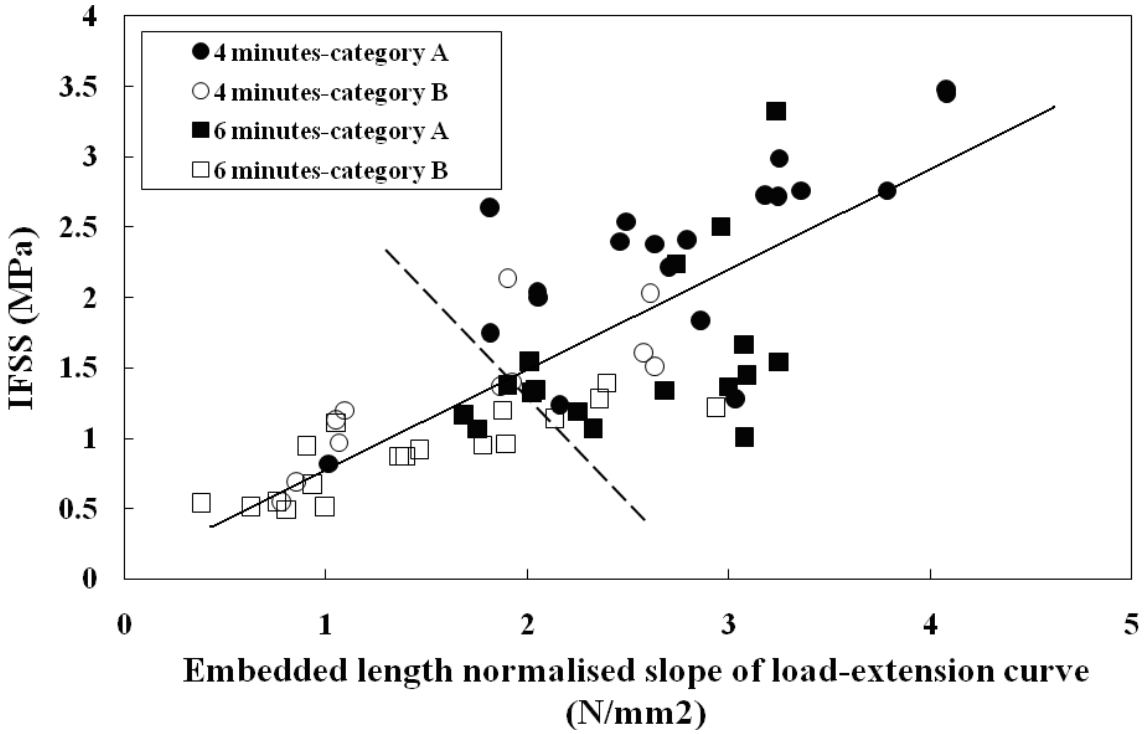

Fig. 15 Comparison of correlation between IFSS and slope of load-extension curve in microbond tests for 4 min and 6 min sets respectively. Dotted and solid lines are drawn to visually distinguish category A & B and 4 min & 6 min data sets respectively.

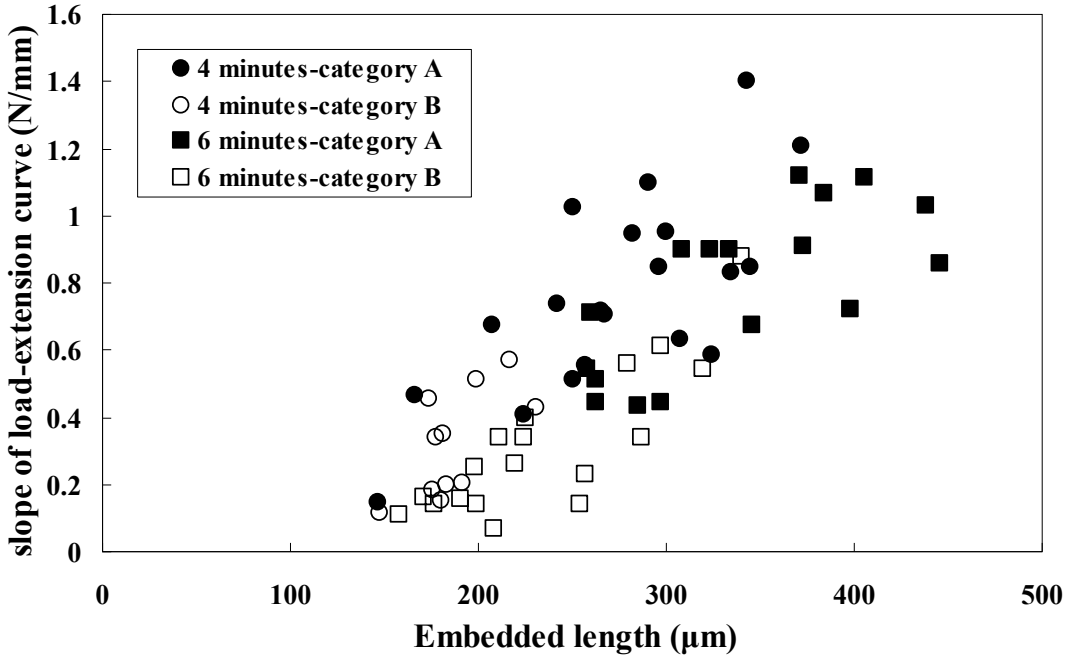

Fig. 16 Slope of load-extension curve vs. embedded length from the microbond test on bare GF-PP47

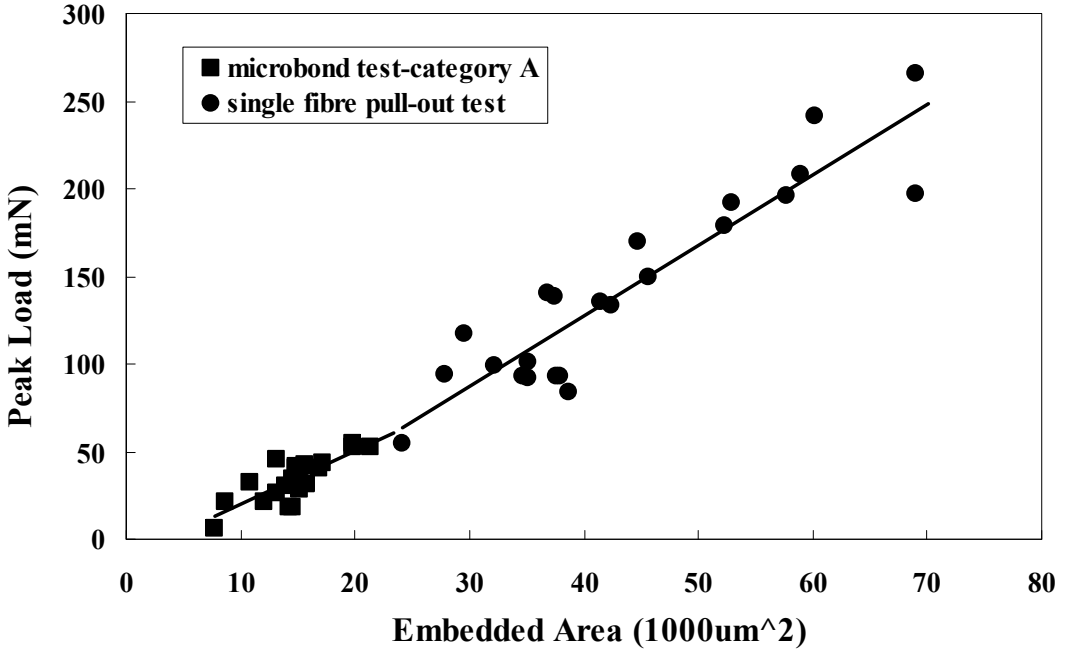

Fig. 17 Peak load vs. embedded area from both microbond and pull-out tests on bare GF-PP47

References

[1] Thomason JL. The influence of fibre length and concentration on the properties of glass fibre reinforced polypropylene: 5. Injection moulded long and short fibre PP Composites: Part A 2002;33:1641-1652.

[2] Thomason JL, Vlug MA. Influence of fibre length and concentration on the properties of glass fibre-reinforced polypropylene: 1. Tensile and flexural modulus Composites: Part A 1996;27(A):477-484.

[3] Thomason JL, Vlug MA. Influence of fibre length and concentration on the properties of glass fibre-reinforced polypropylene: 4. Impact properties Composites: Part A 1997;28(A):277-288.

[4] Mäder E, Freitag K-H. Interface properties and their influence on short fibre composites. Composites 1990;21(5):397-402.

[5] Thomason JL, Schoolenberg GE. An investigation of glass fibre/polypropylene interface strength and its effect on composite properties. Composites 1994; 25(3):197-203.

[6] Drzal LT. The role of the fibre-matrix interphase on composite properties.

Vacuum 1990;41(7-9):1615-1618.

[7] Mäder E, Jacobasch H-J, Grundke K, Gietzelt T. Influence of an optimized interphase on the properties of polypropylene/glass fibre composites. Composites: Part A 1996;27(A): 907-912.

[8] Herrera-Franco PJ, Drzal LT. Comparison of methods for the measurement of fibre/matrix adhesion in composites. Composites 1992;23(1):2-27.

[9] Zhandarov S, Mäder E. Characterization of fibre/matrix interface strength: applicability of different tests, approaches and parameters. Compos. Sci. Tech. 2005;65:149-160.

[10] Broutman.LJ. Measurement of the fibre-polymer matrix interfacial
shear strength. Interfaces in Composites. 1969;ASTM STP 452: 27-41.

[11] Miller B, Muri P, Rebenfeld L. A microbond method for determination of the shear strength of a fibre/resin interface. Compos. Sci. Tech. 1987;28: 17-32.

[12] Ho H, Drzal LT. Evaluation of interfacial mechanical properties of fibre reinforced composites using the microindentation method. Composites: Part A 1996; 27(A):961-971.

[13] Kelly A, Tyson WR. Tensile properties of fibre reinforced metals:
Copper/tungsten and copper/molybdenum Mechanics of Physical

Solids 1965;13:329-350.

[14] Gaur U, Miller B. Microbond method for determination of the shear strength of a fibre/resin interface: Evaluation of experimental parameters. Comp. Sci. Tech. 1989;34: 35-51.

[15] Gonon L, Momtaz A, Hoyweghen DV. Physico-chemical and micromechanical analysis of the interface in a Poly(Phenylene Sulfde)/Glass fibre composite-A microbond study. Polymer Composites 1996;17 (2):265-274.

[16] Moon CK, Lee JO, Cho HH, Kim KS. Effect of diameter and surface treatment of fibre on interfacial shear strength in glass fibre epoxy and HDPE. J. Appl. Polym. Sci. 1992;45:443.

[17] Mäder E, Plsanova E. Characterization and design of interphases in glass fibre reinforced polypropylene. Polymer Composites 2000; 21(3):361-368.

[18] Day RJ, Cauich Rodrigez JV. Investigation of the micromechanics of the microbond test. Compos. Sci. Tech. 1998;58:907-914.

[19] Hoecker F, Karger-Kocsis J. Effects of crystallinity and supermolecular formations on the interfacial shear strength and adhesion in GF/PP composites. Polymer Bulletin 1993;31:707-714.

[20] Pitkethly MJ et al. A round-robin programme on interfacial test methods. Comp. Sci. and Technol 1993;48:205-214.

[21] Thomason JL. Interfacial strength in thermoplastic composites – at last an industry friendly measurement method? Composites: Part A 2002;33:1283-1288.

[22] Craven JP, Cripps R, Viney C. Evaluating the silk/epoxy interface by means of the microbond test. Composites: Part A2000; 31: 653-660.

[23] Landro L. Di, Pegoraro M. Evaluation of residual stresses and adhesion in polymer composites. Composites Part A1996; 27: 847-853.

[24] Wagner HD, Nairn JA. Residual thermal stresses in three concentric transversely isotropic cylinders: application to thermoplastic-matrix composites containing a transcrystalline interphase. Compos. Sci. Tech. 1997;57: 1289-1302.

[25] ASM international. Characterization and Failure Analysis of Plastics. ASM International(OH): 2003.